Heritage Science

RESEARCH

Open Access

The diversity of bronze production technologies during the Eastern Zhou dynasty revealed by analysis of slags from the Baidian and Xincun sites in Central China

Cong Wang[1], Zhenlong Gao[2], Qingzhu Wang[1], Jun Gao[1] and Quanyu Wang[1*]

Abstract

The Eastern Zhou period of China, characterised by complex interactions among vassal states, witnessed significant advancements in bronze production technology. However, the investigation of interactions based on technological comparison among dominant and dependent states remains limited. Focusing on two newly excavated foundry sites, Baidian in Houma, Shanxi, and Xincun in Hebi, Henan, this study provides crucial insights into the bronze production technologies and material sources used by Jin, a major vassal state in Central China, and Wei, a dependent state of Jin, during the Eastern Zhou period. Elemental analysis and microstructural examinations of slags, fragments of crucible wall and furnace wall, show the diversity of bronze production techniques between these two sites: in the Baidian site, bronzes were predominantly produced by co-melting of metallic copper and tin, and remelting of recycled bronzes, whereas in the Xincun site, bronze were probably made by co-melting of copper and tin ore. Furthermore, lead isotope analysis results suggest that the lead materials used for the bronze production at both the sites were likely from the Xiaoqinling region. Integrated with the historical background of complex interactions among vassal states, these findings not only shed light on the technological advancements and resource networks of the Jin and Wei states but also explain the relationships between technology, resources and social dynamics from various perspective. Hopefully this research would promote archeometallurgical study among regions and be applied to other Bronze Age cultures in the world.

Keywords Jin state, Wei state, Slag, Bronze production technology, Lead isotope ratio

Introduction

Bronzes, possessing profound societal and ideological significance, offer a unique window into comprehending the socio-political and economical perspectives of ancient states. The Eastern Zhou era in China, subdivided into the Spring and Autumn period (770–476 BCE), and the Warring States period (475–221 BCE), is a period when numerous vassal states formed alliance and competed with each other, and a period experienced notable advancements in bronze production technology. However, the technological comparison and potential interactions between dominant and subordinate states during this period remains underexplored.

As one of the major powers alongside Qi (齐), Qin (秦), and Chu (楚), the Jin (晋) state was located in an area advantageous for its rich metal resources in the Qinling Mountains and surrounding areas to the south, allowing the Jin to develop a bronze culture with unique regional

*Correspondence:
Quanyu Wang
q.wang@sdu.edu.cn
[1] Joint International Research Laboratory of Environmental and Social Archaeology, Shandong University, Qingdao 266237, Shandong, China
[2] Henan Provincial Institute of Cultural Heritage and Archaeology, Zhengzhou 450000, Henan, China

characteristics. A large number of Jin-related metallurgical remains have been discovered over the years. Among them, the Houma foundry, including Niucun and Baidian locales, is the largest bronze casting site discovered to date in China [1, 2]. The metallurgical remains, especially the clay moulds, indicate that the Jin developed a bronze culture with unique regional characteristics and widely influenced the surrounding vassal states. Despite extensive research on production technology and material sources of bronze ware [3–10], as well as investigations into the decoration, materials and other aspects of the tens of thousands of clay moulds and models with complex shapes and exquisite patterns [11–15], there has been limited exploration of Jin's metallurgical remains, including slags, crucibles and furnace walls. This leads to a limited understanding of the metallurgical technology of the Jin state. Furthermore, whether and how the Jin metallurgical technology had impacted surrounding vassal states remains unknown.

The Wei (卫) state, as a small vassal state adjacent to Jin, often switched between alliance and confrontation with Jin during the Spring and Autumn period, and eventually became a dependent state in the late Spring and Autumn period. Bronze casting remains were unearthed from the Xincun site, the capital of Wei before the invasion of Di (狄人), "barbarian" from the north, in 660 BCE, and became a Jin controlled settlement afterward [16]. The metallurgical remains at Xincun were dated to the transition between the Spring and Autumn period and Warring States period, offering a good case study to investigate the bronze production technology of Wei and the potential impacts from Jin.

Focusing on the metallurgical remains from the Baidian locale of the Houma foundry, and those from the Xincun foundry, this paper presents a preliminary investigation of the melting and alloying technologies and the provenance of raw materials employed by Jin, the dominant state, and Wei, the dependent state, during the Eastern Zhou period. The chemical composition and the microstructures of the metallurgical remains were studied to explore bronze production techniques of the two foundries. fs-LA-MC-ICP-MS was used for lead isotope analysis of metal prills present in the slag samples. This research aims at revealing the technological advancements and resource networks of the Jin and Wei states, thereby exploring the relationship between the selection of bronze production technology and the social dynamics behind it.

Archaeological background

The Baidian foundry site is situated in the northwest of Baidian village in Houma city, Shanxi province, which was the capital of the Jin state during the Eastern Zhou period (770–256 BCE) (Fig. 1a, b) [17]. Located at the political heart of the area, the Baidian foundry remained as a large-scale bronze production centre during the Eastern Zhou period. The foundry at Baidian was discovered during highway construction in 2003, and excavation began in the same year [2]. The excavation area is about 200 m^2 revealing 24 ash pits and 4 tombs, a large number of pottery sherds, and clay moulds/models. Slags and fragments of furnace walls were found in the ash pits. Based on typological analysis, these ash pits were dated to the transition between the Spring and Autumn period and the Warring States period (c. 530–380 BCE) [2]. Thousands of exquisite, decorated clay moulds proved that the Baidian site is an important part of the Houma bronze foundry of Jin.

The Xincun foundry site is in the middle east of Xincun village in Hebi city, Henan province. It was the capital of the Wei state during the Western Zhou period (1046–771 BCE) (Fig. 1a,c). Due to the invasion of the Di in 660 BCE, the Wei state moved its capital eastwards, and its control over the Xincun region was greatly diminished [5]. The site was excavated in 2018, where tombs and bronze-casting clay moulds were unearthed. Slags, furnace/crucible fragments, and clay moulds were found in the ash pits [18]. The Wei occupation of this site can be divided into two phases based on stratigraphy and pottery typology, the early Western Zhou period, and the transition between the Spring and Autumn period and the Warring States period (c. sixth-fifth century BCE). The slags studied here were found from ash pits in the north of the site and date to the second phase [19, 20], when Xincun was no longer the capital of Wei but became a Jin controlled settlement.

Materials and analytical methods

Materials

To better explore the bronze production processes at both the sites and further elucidate the differences and/or similarities between them, a total of 12 samples were selected for this study, including nine pieces from the Baidian site (Tables 1, 2), and three pieces from the Xincun site (Table 3). These samples can be classified as slags, crucibles, and furnace walls. Samples BH2:07, BH2:09, BH20:044, BH20:045, H91:4, and H98:3 was identified as slags, as evidenced by the irregular shape and complete vitrification (Fig. 2a). Metal prills of different sizes were observed on cross-sections of the slags. Samples H210:1, BH2:08, BH17:020, and BH20:043 were likely crucible fragments judged by their relatively small sizes (Fig. 2b). The grey-black vitrified reduction layer generally corresponds to the inner surface, and the porous orange outer surface was exposed to high temperatures. Grey-green rust can be

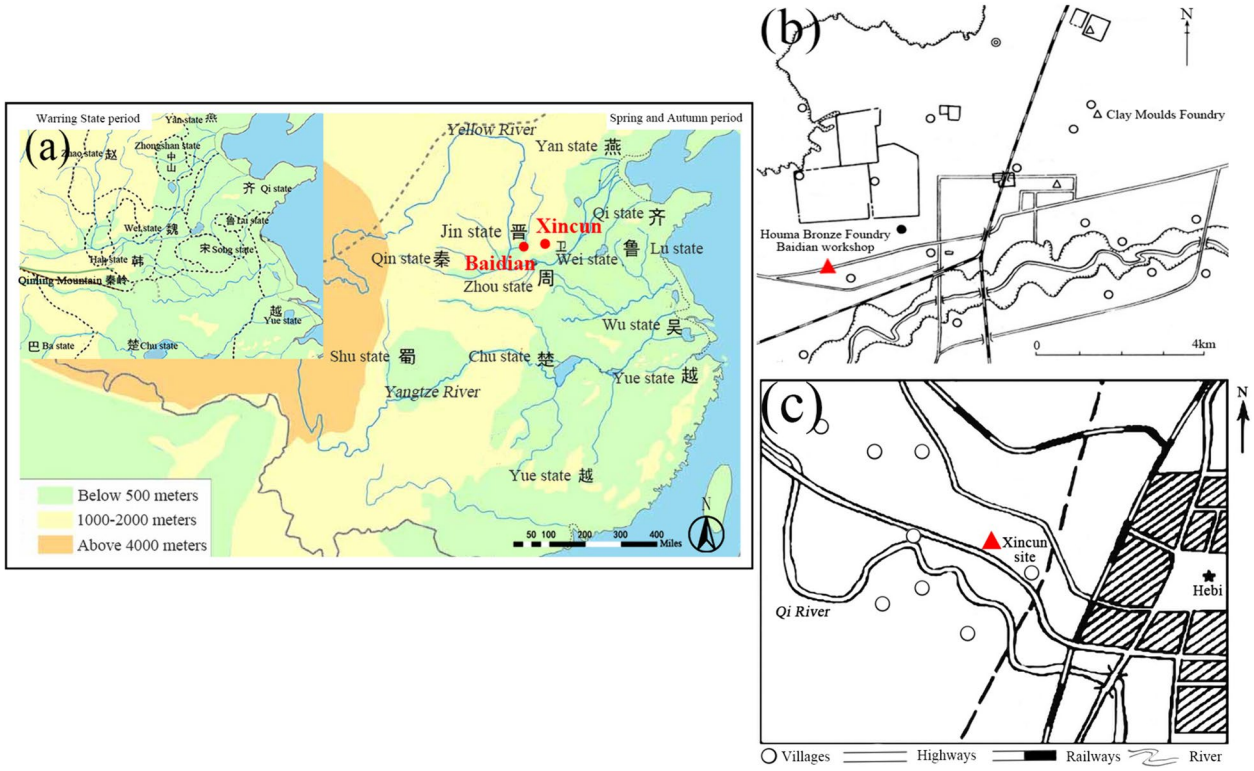

Fig. 1 Maps showing **a** the locations of Baidian, Xincun sites and vassal states mentioned in this paper; **b** Baidian site within the Houma bronze foundry (modified from Shanxi Provincial Institute of Archaeology 2012); **c** Xincun site (modified from Gao et al. 2020)

Table 1 SEM–EDS results of different layers and matrix of the samples from the Baidian site (wt.%)

Sample	Areas of analysis	SiO_2	Al_2O_3	FeO	CaO	K_2O	MgO	Na_2O	CuO	SnO_2	PbO	TiO_2
Crucible BH2:08	Vitrified layer	61.2	17.5	6.0	6.2	3.9	2.5	1.7	–	0.1	–	0.5
	Non-vitrified	63.0	17.9	6.7	4.2	3.6	2.2	1.4	–	0.7	–	0.8
Crucible BH17:020	Vitrified layer	60.4	20.3	8.3	1.2	4.3	2.7	0.9	–	0.3	–	0.9
	Non-vitrified	58.8	20.6	9.1	2.0	4.8	2.7	0.9	–	–	–	0.9
Crucible BH20:043	Vitrified layer	61.4	14.6	4.8	10.8	3.2	2.3	2.0	–	0.2	–	0.9
	Non-vitrified	67.4	13.2	4.9	6.2	3.8	1.8	1.8	–	–	–	0.8
Furnace wall H15:07	Vitrified layer	65.3	14.0	5.7	7.1	2.8	2.1	1.8	–	–	–	0.7
	Non-vitrified	65.2	14.5	5.2	7.6	3.0	1.9	1.6	–	–	–	1.0
Furnace wall H17:017	Vitrified layer	59.8	14.3	5.3	13.0	3.2	2.2	1.7	–	–	–	0.7
	Non-vitrified	62.1	14.6	5.6	9.8	2.9	2.2	1.7	–	–	–	1.1
Slag BH20:044	Vitrified matrix	34.2	6.6	13.5	36.0	1.6	2.7	0.7	3.4	0.6	0.1	0.8
Slag BH2:07	Vitrified matrix	67.1	13.5	4.4	8.4	2.9	1.8	1.4	–	–	–	0.5
Slag BH20:045	Vitrified matrix	63.7	12.6	3.8	9.3	2.3	2.5	2.1	2.0	0.2	1.2	0.5
Slag BH2:09	Vitrified matrix	60.7	11.8	3.4	12.9	2.4	2.1	2.0	1.9	0.2	1.9	0.8

seen on the surface of the vitrified layer, pointing it to probable metal melting activities. Samples H17:017 and H15:07 were probably furnace walls rather than crucibles as they were thicker and coarser (Fig. 2c) [21]. The cross-section of both the samples showed a multi-layered interior part, and elongated voids can be identified within the ceramic body. The thin vitrified layer on the surface suggests that they have probably been used for numerous times.

Table 2 SEM–EDS results on metal prills in the slags from the Baidian site (wt.%)

Sample	No	Cu	Sn	Pb	Fe	As	S	O	Other	Identification
Slag BH2:07	1	62.7	0.3	0.2	3.2	–	26.1	7.4	–	Copper sulphide
Slag BH20:044	1	75.8	18.8	0.4	0.9	–	–	4.0	–	Tin bronze
	2	84.5	12.6	0.7	0.6	–	–	1.4	–	Tin bronze
	3	56.5	38.2	0.1	1.5	–	–	3.7	–	Tin bronze
	4	68.3	25.0	0.2	1.3	–	–	5.2	–	Tin bronze
	5	18.9	43.1	0.7	7.5	–	0.5	29.2	–	Tin bronze
	6	67.3	26.0	0.3	1.3	–	–	5.0	Sb:0.2	Tin bronze
	7	79.6	17.9	0.1	0.4	–	–	1.7	–	Tin bronze
Slag BH20:045	1	70.0	17.8	3.9	0.1	1.7	–	6.4	–	Bronze prill
	2	4.5	2.1	70.2	0.2	1.2	–	17.5	Ag:4.4	Silver-containing prill
	3	1.4	2.7	84.3	–	1.4	–	10.2	–	Lead-rich prill
	4	–	98.2	0.5	0.4	–	–	0.9	–	Tin prill
	5	92.9	2.4	1.4	–	–	–	3.2	–	Bronze prill
	6	88.6	3.5	3.5	0.1	0.8	–	3.6	–	Bronze prill
	7	87.2	5.4	5.1	–	–	–	2.3	–	Bronze prill
	8	61.4	4.5	6.4	0.4	–	–	27.2	–	Bronze prill
	9	7.1	45.6	7.8	0.5	–	–	39.0	–	Bronze prill
Slag BH2:09	1	85.6	7.6	2.8	–	–	–	3.5	Sb:0.4	Bronze prill
	2	6.6	2.7	58.2	0.4	1.7	–	23.8	Sb:0.5; Cl:6.1	Bronze prill
	3	2.7	2.4	60.1	1.7	1.5	–	31.6	–	Bronze prill
	4	4.4	4.4	65.5	1.0	1.4	–	23.5	–	Bronze prill
	5	45.3	2.1	33.1	0.5	1.3	–	18.0	–	Bronze prill
	6	0.5	0.7	75.0	0.6	1.2	–	22.0	–	Lead prill
	7	0.7	0.3	74.0	0.4	–	–	22.5	–	Lead prill
	8	1.3	1.7	72.9	0.5	1.5	–	22.2	–	Lead prill
	9	1.1	1.9	70.9	0.5	1.8	–	23.7	–	Lead prill
	10	0.8	1.9	72.2	0.6	1.7	–	22.9	–	Lead prill

Table 3 SEM–EDS results of different layers and matrix of the samples from the Xincun site (wt.%)

Sample	Areas of analysis	SiO_2	Al_2O_3	FeO	CaO	K_2O	MgO	Na_2O	CuO	SnO_2	PbO	TiO_2
Crucible H210:1	Vitrified layer	69.5	14.9	7.0	1.6	3.3	1.4	1.2	–	0.4	0.2	0.5
	Partly vitrified	69.7	15.0	6.2	1.9	3.3	2.0	1.7	–	0.4	0.2	0.5
	Non-vitrified	69.6	15.9	5.1	1.6	3.5	2.0	1.8	–	0.2	0.1	0.2
Slag H91:4	Vitrified matrix	63.3	16.4	6.2	2.1	4.2	2.3	1.5	1.5	0.8	0.3	1.3
Slag H98:3	Vitrified matrix	36.4	6.3	1.5	26.7	0.7	2.1	0.7	1.9	13.1	4.2	0.2

Analytical methods

Each sample underwent comprehensive analyses, including macro- and micro-scale observations, metallographic analysis, chemical compositional analysis, and in situ micro-analysis of lead isotopes. Macroscopic observations of all the samples were conducted using a Leica DVM6M digital microscope, the metallographic structure of the samples was observed and documented using a Leica DMi8 metallurgical microscope. Microstructure and the chemical analysis were conducted using a Thermo Scientific Quattros scanning electron microscope coupled with a Bruker Xflash 6160 energy dispersive X-ray spectrometer (SEM–EDS). The in situ micro-analysis of lead isotopes for metal prills embodied in slags were conducted using, a Nu PlasmaII multi-receiver inductively coupled plasma mass spectrometry equipped with a NWR UP^{Femto} femtosecond laser ablation system (fs-LA-MC-ICP-MS).

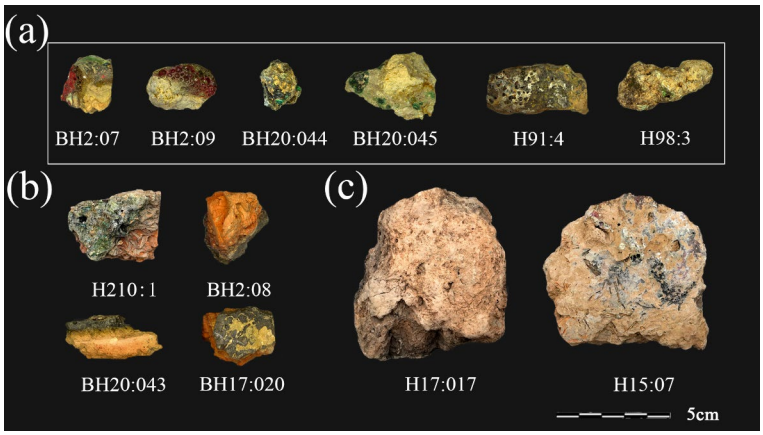

Fig. 2 Slags, crucibles, and furnace wall fragments from the Baidian and Xincun foundry sites. **a** Slags, including H91: 4 and H98:3 from the Xincun site and the rest from the Baidian site; **b** Crucibles, including H210:1 from the Xincun site and the others from the Baidian site; **c** Furnace walls from the Baidian site

Metallographic samples were taken by cutting the slags to include, to the greatest extent possible, all the different layers, including the vitrified and unvitrified sections. The samples were then mounted in epoxy resin, ground with sandpaper of different grit sizes (600–1200), and subsequently polished to a finish of 0.25 μm with diamond pastes. After initial observations of the structure, including inclusions, the polished samples were etched using a 3% alcoholic ferric chloride solution, to reveal the metallographic structure of the metal prills.

The SEM–EDS analyses were for the examination of the microstructure and the chemical composition of the matrix, mineral phases, and metal prills of the samples. The analyses were conducted at an accelerating voltage of 20 kV at a low vacuum (50 Pa), with a working distance of 8.5 mm and a scanning time of 90 s. The detection limits for each element varies but generally fall within the range of 0.1%~0.3%. The chemical composition results were obtained by taking an average of 3 areas of analyses for each analysed sample. For the matrix, the analysed areas were selected to avoid metal prills, unreacted inclusions and mineral phases. For the mineral phases and metal prills, given the heterogenous microstructure of the samples, the compositional analyses were performed at the magnification as large as possible. The results of chemical analyses were presented as stoichiometric oxides and have been normalised to 100% by weight (wt.%). The chemical composition of mineral phases numbered in SEM images was shown in the Supplementary Material (Table S1 and S2). All SEM images in this paper are backscattered electron images.

In this study, fs-LA-MC-ICP-MS was used to conduct in-situ micro-area determination of Pb isotopes on metal prills present in the slag samples. The application of this analytical technique has been validified by experiments [22–24]. Four slag samples were examined, in which a total of 21 metal prills with different compositions were analysed. The MC-ICP-MS adopted TRA (Time-Resolved Analysis) mode, while the Laser ablation adopted line scanning method. The integration time for TRA mode was about 0.2 s, and the scanning speed was 5 μm/s. The gas background blank acquisition time was 30 s, and the sample signal acquisition time was 50 s. The scanning length for LA line scanning method was 120 μm, and different spot sizes were selected according to the Pb content of the sample. For areas with high-concentration of lead, the spot size was set to 9-20 μm, while for areas with low level of lead, the spot size was set to more than 30 μm to obtain higher Pb intensities. Certified reference GBW02137 was used to check the analytical accuracy. The relative errors of $^{208}Pb/^{204}Pb$, $^{207}Pb/^{204}Pb$ and $^{206}Pb/^{204}Pb$ ratios were less than 0.05% [25].

Results and discussion

The nature of slags from the Baidian site

Comparing the composition of technical ceramics with that of associated slags is an effective means to indicate whether slag oxides derived from the melted ceramics or contributed by the metallurgical materials [26]. SEM–EDS results of different layers and matrix of the samples are shown in Table 1. Both the vitrified layer and the non-vitrified area of the crucibles, furnace walls were composed of high silicon (Si) and aluminium (Al) contents, indicating that the vitrified sections were partially molten crucible or furnace walls. The significantly high calcium (Ca) contents for the vitrified areas of the crucible BH2:08, BH20:043, and furnace H17:017 were

possibly a result of contact with fuel ash. Small amounts of tin (< 1%) were detected in crucibles BH17:020 and BH20:043, while no tin oxides were observed in them. Slag layer was absent in the crucible and furnace walls; a metal-rich grain containing 68.8% Ba, 21.6% Fe, and 9.6% Sn was found in crucible BH20:043 (Fig. 3a).

Copper refining or melting

The SEM–EDS analysis of the four slag samples from the Baidian site revealed that only slag BH2:07 consists of a single copper sulphide prill, without tin or lead being detected (Table 2). The vitrified matrix of this slag has higher silicon and aluminium contents, lower iron (Fe) and calcium, and no detectable bronze metal elements. These features confirm that slag BH2:07 was relevant to copper metallurgy.

As early as by the Erlitou period, the southern Shanxi region had established a bronze industry with separation of mining, smelting and casting. Several early mining sites and smelting sites discovered are concentrated in and around the Zhongtiaoshan mining area [27, 28]. Thus, as a bronze workshop far away from the mining area, the Baidian site was unlikely to have conducted primary smelting. While the slag is heterogeneous and very small, making the absence of iron-and copper-bearing phases (i.e., magnetite, wüstite) in this sample, which are important indicators for judging refining or melting. As such, it is not possible to conclude whether BH2:07 resulted from refining or melting.

Co-melting of fresh metals

Slags BH20:044 and BH20:045 from the Baidian site were related to bronze production. All the metal prills in the slag BH20:044 were tin bronzes (tin content 12.6–43.1%) (Table 2). Some prills were found to contain a small amount of iron (0.4–7.5%) and antimony (Sb) (< 2%), which were most likely originated from the ore or soil impurities rather than deliberate additions to the alloy.

Slag BH20:044 was characterised by significantly higher calcium and iron content in its matrix composition (Table 1), which is commonly regarded as an indicator of mineral involvement in the alloy. But the conspicuous absence of cassiterite and copper oxides in the oxide phases indicated slag BH20:044 probably resulted from the co-melting of metallic copper and tin. The iron silicates (containing 64.6% Fe, 31.4% O and 4.0% Si, probably corresponding to $3FeO{\blacksquare}SiO_2$) found in the matrix often encapsulate bronze prills (Fig. 3b), seem more consistent with the oxidation of metallic iron contained within the bronze prills than with the gangue materials [26]. This also support the speculation that metals rather than minerals were adding to the alloy system.

Additionally, the most of the iron may have derived from the tin materials, as evidenced by the higher iron content in high-tin bronze prills, compared to

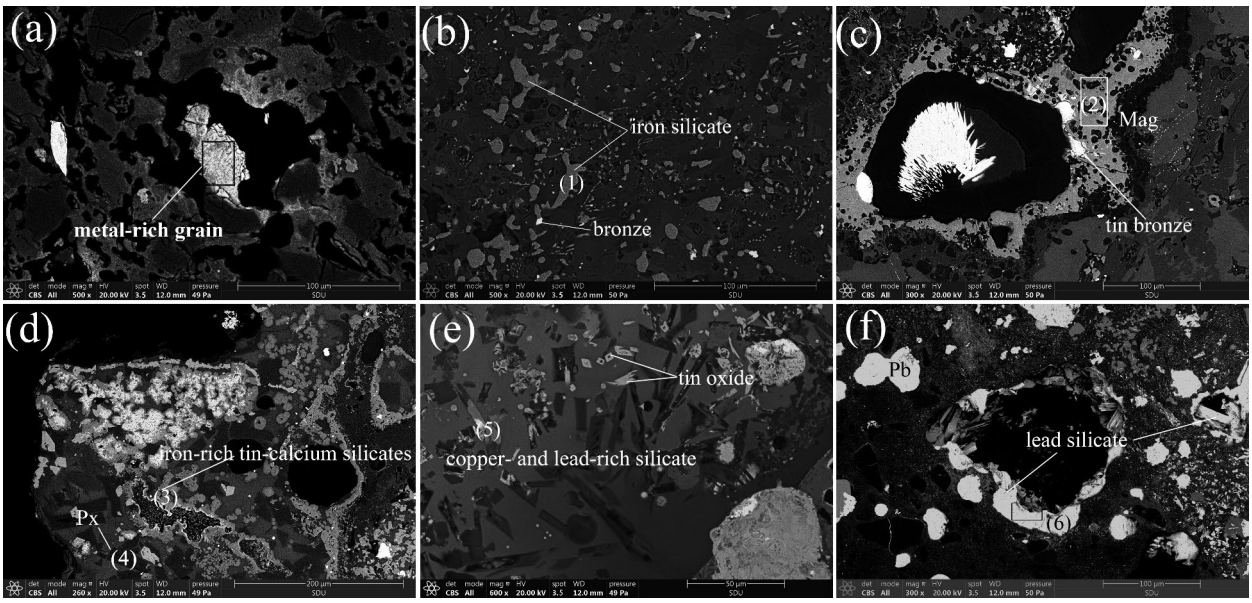

Fig. 3 SEM backscattered electron images of different areas and mineralogical assemblages of slags from the Baidian site. The chemical composition of mineral phases numbered in the images were listed in the Supplementary Material (Table S1). **a** Metal-rich grain containing Ba- and Sn-rich inclusions in crucible BH20:043; **b**-**d** The matrix of slag BH20:044, showing the presence of iron silicates, magnetite (Mag), iron-rich tin-calcium silicates, and calcium-rich pyroxene (Px) embedded in the matrix; **e** Tin oxide, copper- and lead-rich silicates in slag BH20:045; **f** Lead silicates in the centre of slag BH2:09

copper-rich prills. This means that the tin metal used in the alloy is not pure, which is also reflected in crucible BH20:043. The free enthalpy for tin and iron to form silicates are very close, making their separation difficult, and prone to the formation of Sn_2Fe or SnFe during tin smelting [29]. The presence of magnetite (containing 30.0% O, 70.0% Fe, corresponding to Fe_3O_4) in the slag further supports the association of iron with tin (Fig. 3c). Magnetite shares similarities with cassiterite in terms of density and luster, therefore, it could have been mistakenly taken as cassiterite as a part of the gangue [30].

A relative abundance of calcium-rich pyroxene and iron-rich tin-calcium silicates were also found in the matrix (Fig. 3d). With elevated calcium concentration, potentially introduced by fuel ash or fluxes, the calcium-rich silicates were likely formed from the combination of tin-iron oxides with calcium-rich minerals under a weak reducing atmosphere during melting or cooling [31].

Moving on to slag BH20:045, most of the metal prills in this sample were Cu-Sn–Pb phases. The tin contents in slag BH20:045 varied widely, ranging from 1.0% to 98.2%, suggested that metallic tin or cassiterite was added to alloying process rather than waste bronzes [30, 32–34]. A few high-lead bronze prills contained arsenic (As, 1.2–1.7%), silver (Ag, 0.2–4.4%) and traces of antimony (0.8–1.1%), which should be impurities in the lead material.

The vitrified matrix composition of this slag was similar to that of technical ceramics, with an average calcium content of ~ 10%, and an iron content of ~ 3% (Table 1). Slag BH20:045 may represent a co-melting process involving tin, copper, and lead. The tin addition is more likely in metallic form, as evidenced by the microstructure of tin oxide crystals, which are characterised by acicular, rhombic and skeletal shapes (Fig. 3e), along with the low iron content observed in the slag compositions [35]. The presence of copper or lead silicate is commonly regarded as an indicator of copper or lead mineral involvement in the alloy (Fig. 3e) [26]. However, the enrichment of copper-lead silicate in this sample was likely resulted from the use of a copper-rich lead ingot. A batch of lead ingots with up to 10.2% Cu were found at the Houma foundry (containing 71.6% Pb, 0.8% Sn, 0.9% Fe), which was believed to be a by-product of smelting copper-lead polymetallic ores [36]. Such lead ingots could have been used in the co-melting process which produced slag BH20:045. Hence, the presence of tin, lead and copper in the form of oxide inclusions reflects varying degrees of oxidation of the molten metal during melting [37].

Melting of recycled metals

The possible re-melting process, i.e., the use of waste metals to produce new artefacts is represented by slag BH2:09. Most of metal prills in slag BH2:09 were Cu-Sn–Pb bronze, but numerous lead prills were also trapped within the matrix. Compared to other samples (e.g., BH20:044 and BH20:045), the metal prills in this slag had a narrow range of tin content (0.3–7.6%) (Table 2). The standard deviation (SD) of tin concentrations for metal prills in BH2:09 is 2.1, while that in BH20:044 and BH20:045 are 11.1 and 32.5, respectively. The narrow tin concentrations in the metal prills and the lack of extraordinary high tin content (Sn > 40%) suggest that metallic tin or cassiterite was unlikely added to alloying process [30, 32–34]. The use of recycled metals was not unusual in bronze workshops of the Jin state. For example, a small number of metal blocks, likely waste bronzes, were found in the Houma foundry [17]. The lead isotope data of the prills in BH2:09 also support the use of recycled metals. Pollard [38] established a mixing model for lead isotopes, pointing that the lead isotopic ratio of the mixture is a linear function of the reciprocal of lead concentration of the mixture. As shown in Fig. 4, compared to the slag BH20:045, the $^{206}Pb/^{204}Pb$ ratios of the prills in BH2:09 appears linear to the reciprocals of the corresponding lead concentrations, suggesting a possible mixture. Since the source of lead material in Jin was relatively consistent during this period, this mixing could have been due to the use of recycled metals.

The matrix of this slag is formed by Ca-Al silicate with richer copper and lead content (1.9%), but small amount of tin dissolved in it (Table 1). The significant quantity of lead silicate crystals was also observed in the slag, possibly contributing to the increased lead content in the matrix (Fig. 3f). The presence of a large amount of lead prills and lead silicate in slag BH2:09 does not rule out the possibility that fresh lead materials were added during remelting.

The nature of slags from the Xincun site

The SEM–EDS results of different layers and matrix of the samples from the Xincun site are shown in Table 3. The microstructure of crucible H210:1 showed the presence of a vitrified layer, a partly vitrified region, and a nonvitrified area (Fig. 5a–c). The vitrified layer was characterised by high silicon and aluminium, along with moderate iron, and comparatively low calcium contents. This composition is generally consistent with that of the nonvitrified region, albeit with a slightly higher iron content. The elevated iron in the vitrified layer probably resulted from the direct contact between the crucible wall and molten metal. No metallic prills were observed within the vitrified layer, but a small amount of metal containing 65.4% Pb, 15.2% Fe, 10.6% As and 8.8% Sn was found (Fig. 5a).

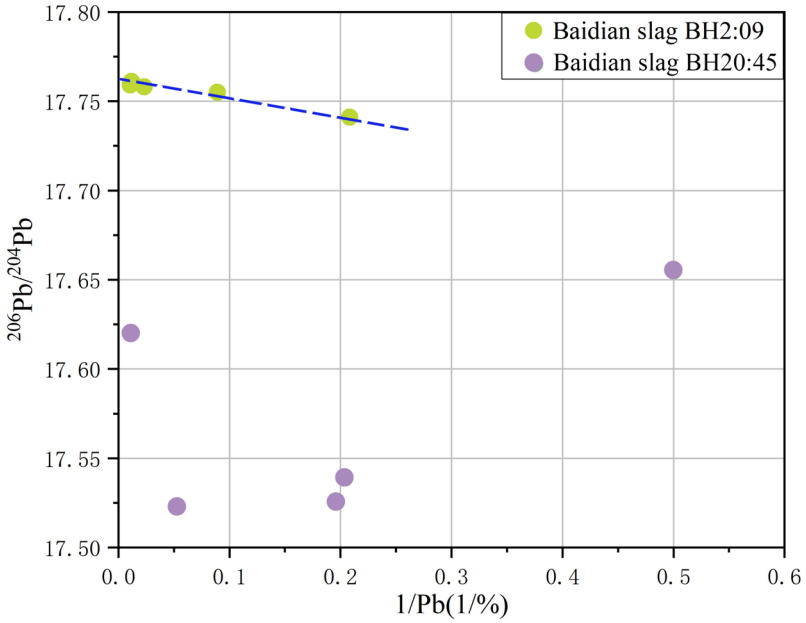

Fig. 4 1/Pb-lead isotope ratio chart of Baidian slags BH2:09 and BH20:045

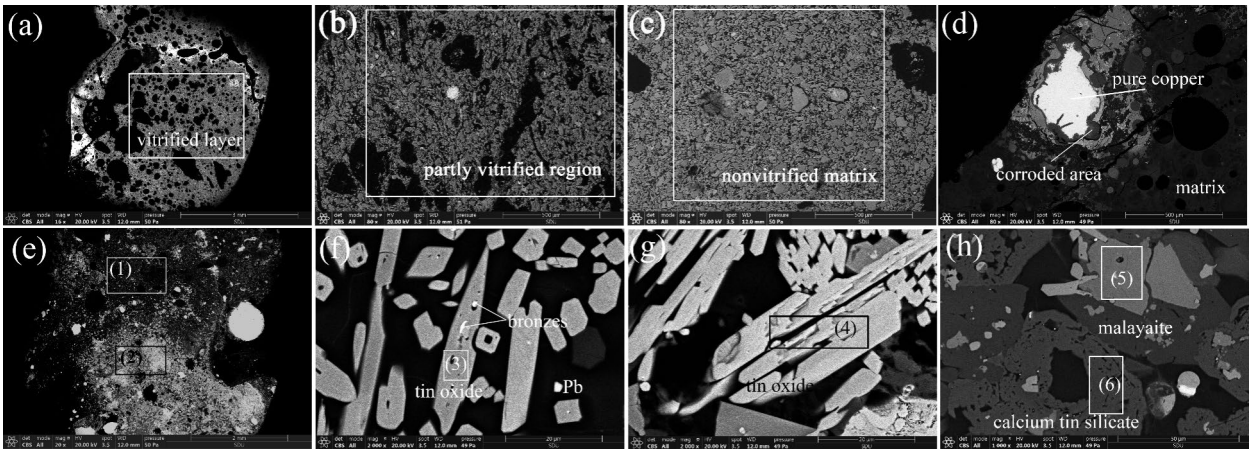

Fig. 5 SEM backscattered electron images of the crucible and slags from the Xincun site. The chemical composition of mineral phases numbered in the images were listed in the Supplementary Material (Table S2). **a**-**c** Micrographs of different parts of crucible H210:1; **d** Metal prills in slag H91:4; **e**–**h** H98:3; **e** Heterogeneous matrix of slag H98:3; **f** Hollow tin oxide encrusted with bronze; **g** Well-developed tin oxide; **h** Malayaite and calcium tin silicate

Table 4 SEM–EDS results on metal prills in the slags from the Xincun site (wt.%)

Sample	No	Cu	Sn	Pb	Fe	As	O	Identification
Slag H91:4	1	95.9	0.2	0.5	0.2	–	3.3	copper prill
Slag H98:3	1	84.1	10.7	3.0	0.2	1.0	1.0	bronze prill
	2	46.8	40.1	9.3	0.2	0.8	2.8	bronze prill

Copper melting

The metal prills in slag H91:4 was irregular in shape, and were identified as copper prills with Cu_2O inclusions (Fig. 5d), comprising approximately 95.9% Cu (Table 4), with trace amounts of tin, and lead as impurities. The matrix composition of slag H91:4 is quite similar to that of the vitrified layer in crucible H210:1, characterised with high silicon and aluminium content. This indicated that the silicon and aluminium content in the slag mainly come from technical ceramic rather than ores. A higher level of copper and iron were also detected in the matrix (Table 3).

The copper and iron concentrations in this slag initially points it to a refining slag, because refining slag usually contain large amounts of iron oxide (i.e., magnetite, wüstite) due to the oxidation of iron and other impurities in copper [39]. However, the moderate copper and iron concentrations (both below 10%), and the absence of Fe-bearing phases in the slag suggest that the iron in the slag more likely resulted from re-oxidation of iron impurity in raw copper, alongside potential contributions from the crucible. Slag H91:4 is more likely associated with melting processes. The possibility of melting is also supported by the presence of cuprite (Cu_2O) inclusions. These phases are commonly associated with copper melting practices rather than refining activities, as they typically form from the oxidation of metallic copper [40–42].

Co-melting tin minerals with metallic copper

The nature of the slag H98:3 is quite different from slag H91:4. Almost all of the metal prills of varying sizes in slag H98:3 was identified as bronze prills, with the tin contents ranging from 10.7% to 40.1% (Table 4). The vitrified matrix is enriched in both tin and lead content, and higher calcium content was also detected in this slag (Table 3).

H98:3 likely represents co-melting tin-rich minerals with metallic copper. The microstructure of slag H98:3 was heterogeneous, with different zones having varying mineralogical compositions (Fig. 5e). The large amount of tin in the matrix reflects what microscopically observed: various tin-rich phases concentrated near the metal prills. Two types of tin oxide crystals were identified in this sample. Type I are in the needle-like or plate-like form, some with hollow cores enclosing bronze prills (Fig. 5f), which are undoubtedly produced by the oxidation of tin in the bronze prills. While type II are in the cluster shape and developed well (Fig. 5g), could potentially formed through the recrystallisation of unreduced tin ore (sometimes with significant Ta/W/Nb content). Alternatively, its formation could also be attributed to localised oxidation of bronze prills [35]. However, as Rademakers and Farci suggested, the crystal form of tin oxide alone is insufficient to confirm a specific alloy technology. Instead, it serves to provide a reference for distinguishing different tin bronze production processes [35].

Another potential piece of supportive evidence for the utilisation of tin ore in the alloying process is the large calcium content in this sample. Calcium tin silicate, and malayaite (CaSn (SiO_4) O) formed through the reaction between tin oxide and calcium-rich pyroxenes were found in the slag (Fig. 5h) [43]. The presence of newly formed Ca-Sn and Ca-Sn-Si compounds around tin oxide crystals (Fig. 5h) indicates that tin entered the system in mineral form [44]. The large calcium content could have been from gangue given the low calcium content in the crucible. Although tin ores are characterised by a variety of deposit types and cassiterite is generally pure, skarn deposits of tin account for more than 80% in China and are distributed in Inner Mongolia, Hunan, Jiangxi, Yunnan, Guangxi and Guangdong [45, 46]. The main component of skarn deposit is gangue, which mainly contains calcium, magnesium and iron. Geological analyses of tin mines in Inner Mongolia, Hunan and Jiangxi show that the gangue is mainly composed of marble, dolomite, diopside and fluorite, which are calcium-bearing minerals [47–49]. Archaeological studies have also found that some of the smelting slags from the Habaqila site, Keshketengqi, Inner Mongolia, have a high calcium content. The calcium content of the slags is probably attributed to fluorite in tin-bearing polymetallic ores found at the site [50]. However, the uneven enriched calcium could also come from fuel ash or flux, although the latter is less likely, because calcareous fluxes such as limestone ($CaCO_3$) or dolomite (CaMg (CO_3)$_2$) have not yet been found from pre-Qin bronze foundries.

To further investigate whether tin ore was employed during the alloying process, we compared the tin contents of bronzes from the Jin state [5–7, 51–54]. The assumption is that co-melting copper ingots and tin ore would make it more challenging to control the alloy composition, leading to a broader range of tin content in bronzes. Conversely, co-melting metal ingots facilitates easier control of the alloy composition, resulting in a narrower distribution range of tin content in bronze alloys. Considering that the Rite of Zhou·Kaogongji provided a series of six "Cu-Sn" recipes for the manufacture of specific types of bronze object [55], and since bronze vessels were the main type of bronze production in Jin, only the tin content data for the bronze vessels were used to explore the range of tin content over time, and they are presented in Table S3 and Fig. 6. As shown in Fig. 6, the distribution range of tin content of bronze vessels from various sites becomes smaller from the late Western Zhou to the Spring and Autumn period, reflecting that craftsman had a better control of tin content of bronze

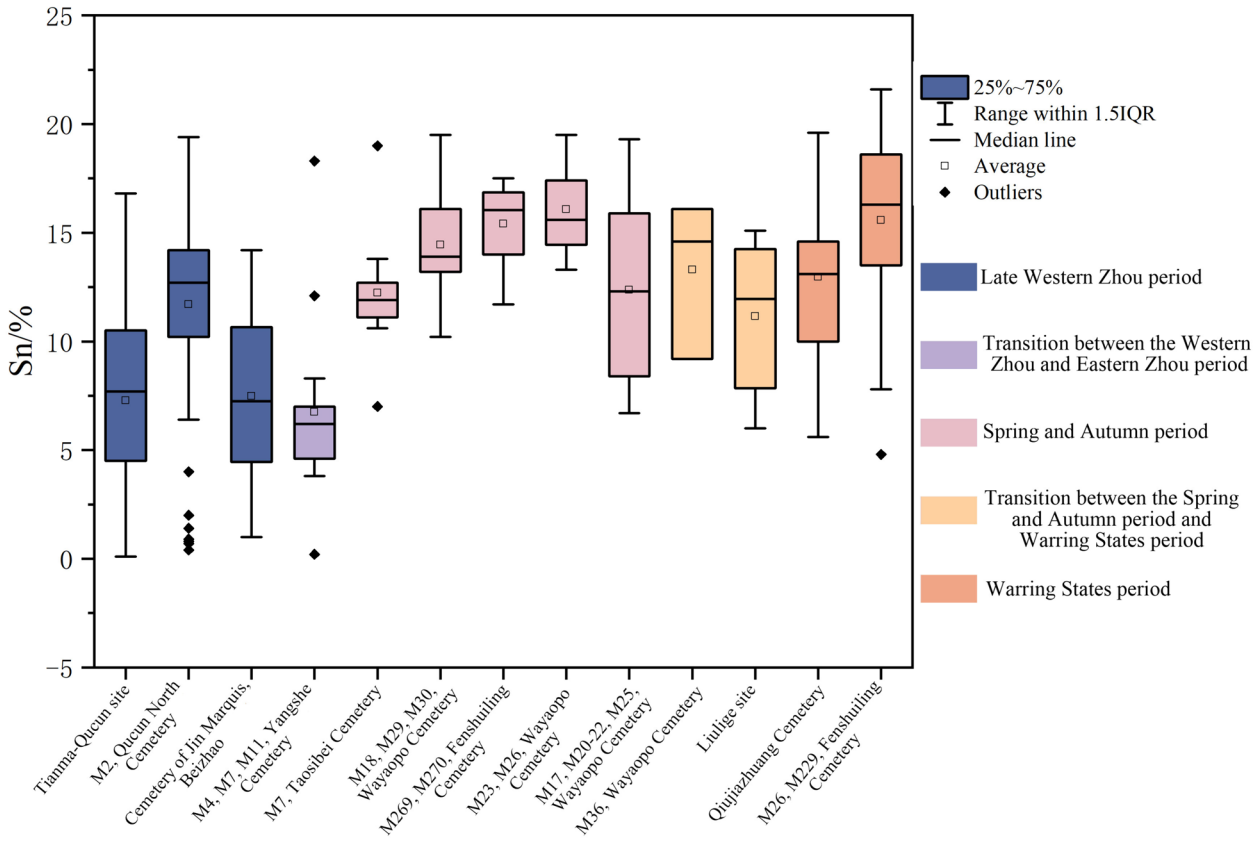

Fig. 6 Changes of tin content in bronzes from Jin state with time

vessels in early Eastern Zhou period. However, from the late Spring and Autumn period to the Warring States period, the tin content of bronze vessels varies widely regardless sites and the type of vessels, indicating a shift in alloying technology. Although the apparent difference in tin content in Fig. 6 may be the result of mixing different types of bronze vessel or using recycled metals, using tin ore for bronze production cannot be ruled out.

Sources of materials in the Baidian and Xincun sites

The results of lead isotope analyses on metal prills with different compositions in the selected slags are shown in Table 5. For Baidian slag BH20:045, five prills, with lead contents ranging from 2.0% to 89.4%, were analysed. As shown in Fig. 7, the lead isotope distribution of the bronze prills with low-lead (≤2%) in Baidian slag BH20:045 is significantly different from that of the bronze prills with high-lead (>2%). It is likely that the prills with ≤2% lead represent the source of copper. The lead isotope ratios of the high-lead prills exhibited a linear distribution, consistent to the data from a lead ingot discovered at the Houma foundry site. In contrast to slag BH20:045, the lead isotope ratios of prills in slag BH2:09 are relatively concentrated.

For Xincun slag H98:3, the lead isotope ratios of either high- or low-lead prills showed apparent linear distribution, which could be attributed to two possible explanations. One possibility is that the copper and lead materials may come from the same source. The other possibility is that the low-lead prills may have been contaminated by lead materials. Therefore, this study chose the lead isotope ratio of high lead prills to represent the source of lead for provenance study.

The lead content in Baidian slag BH20:044 is below 2%. Given that the lead content in tin ore is typically lower than that in copper ore, and considering the weak lead isotope signal in tin ore, it is more likely that the lead isotope ratio in this sample represents the source of the copper material [56, 57]. However, caution should be taken regarding the potential contamination from lead during the alloying and casting process [58, 59].

Metal resource networks of the Baidian and Xincun sites

During the Eastern Zhou period, various vassal states were constantly at war with each other, and cultural exchanges were very common. To explore the circulation of bronze materials between the Baidian site, Xincun site and other vassal states, the lead isotope ratios of

Table 5 Lead isotopic ratios and main components of metal prills within the slags from the Baidian and Xincun sites

Site	Sample	Lead isotopic ratios					Main components (wt.%)		
		$^{208}Pb/^{204}Pb$	$^{207}Pb/^{204}Pb$	$^{206}Pb/^{204}Pb$	$^{208}Pb/^{206}Pb$	$^{207}Pb/^{206}Pb$	Cu	Sn	Pb
Xincun	H98:3	38.205	15.611	17.726	2.155	0.880	84.2	10.7	5.1
		38.072	15.565	17.682	2.153	0.880	72.9	21.5	5.6
		38.187	15.596	17.714	2.154	0.880	77.7	17.6	3.8
		38.197	15.600	17.718	2.156	0.880	70.3	24.4	5.3
		38.083	15.573	17.708	2.151	0.880	71.5	24.5	4.0
		38.042	15.555	17.676	2.152	0.880	59.7	28.0	12.3
		38.000	15.546	17.671	2.150	0.880	82.2	15.5	2.3
		38.082	15.571	17.695	2.151	0.880	79.0	19.3	1.7
		37.994	15.567	17.680	2.149	0.880	84.7	13.7	1.0
		38.052	15.567	17.688	2.151	0.880	60.7	37.9	1.5
Baidian	BH2:09	38.524	15.610	17.741	2.170	0.880	87.6	7.6	4.8
		38.544	15.628	17.755	2.171	0.880	79.9	8.9	11.2
		38.569	15.636	17.761	2.171	0.880	14.8	1.3	83.9
		38.554	15.631	17.758	2.171	0.880	54.8	2.4	42.8
		38.560	15.629	17.759	2.171	0.880	2.3	4.6	93.2
	BH20:044	38.228	15.645	17.794	2.149	0.880	72.1	26.3	1.6
	BH20:045	38.041	15.565	17.523	2.171	0.888	64.5	16.6	18.8
		38.210	15.609	17.620	2.171	0.887	3.2	3.2	89.4
		37.952	15.551	17.526	2.165	0.888	91.4	3.5	5.1
		38.089	15.729	17.655	2.154	0.889	96.7	1.3	2.0
		38.060	15.584	17.539	2.170	0.889	89.7	5.4	4.9

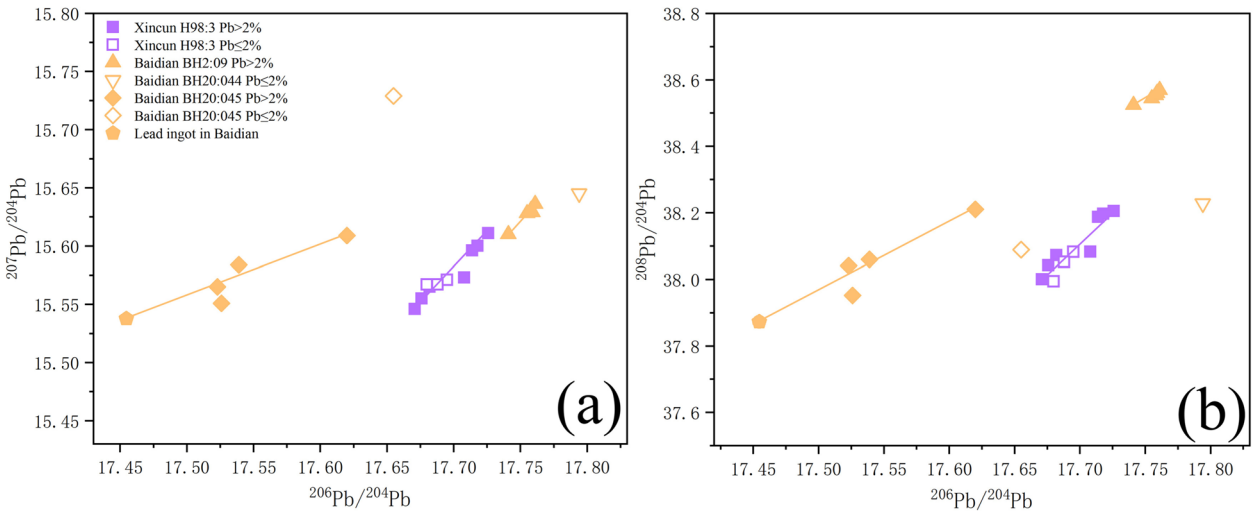

Fig. 7 Plots of lead isotope ratios of the Baidian and Xincun slags, **a** $^{207}Pb/^{204}Pb$ versus $^{206}Pb/^{204}Pb$; **b** $^{208}Pb/^{204}Pb$ versus $^{206}Pb/^{204}Pb$

the slags studied here from the two sites were compared with available data of bronzes from the Jin, Han, Qi, Qin, Xue (薛), Chu, Yue (越), Zeng (曾), and Shu (蜀) states during the transition between the Spring and Autumn period and Warring States period (Fig. 8) [51, 60–67]. Taking leaded bronzes (with ≥ 2% Pb) into consideration (Table S4; Fig. 8a, b), it was found that the bronzes from different regions at this time overlapped to varying degrees, but had obvious regional characteristics. In addition to Jin, the data of the Xincun and Baidian sites also overlap with some data of Qi, Xue, Han, Chu, and Zeng bronzes. We can assume that the lead isotope ratios

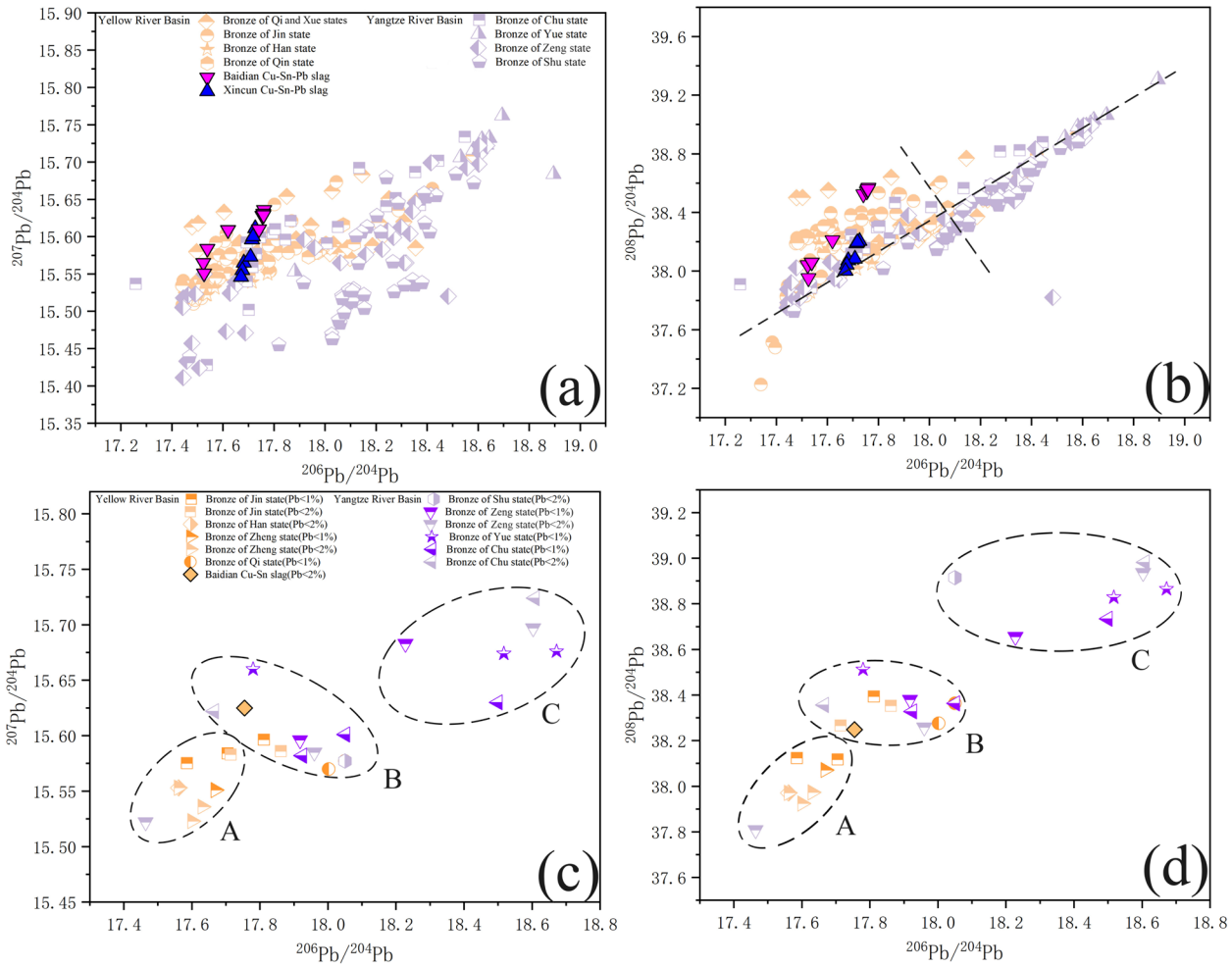

Fig. 8 The binary image of $^{207}Pb/^{204}Pb$ versus $^{206}Pb/^{204}Pb$, and the binary image of $^{208}Pb/^{204}Pb$ versus $^{206}Pb/^{204}Pb$ for slags from the Baidian and Xincun sites. **a**, **b**: Comparison with leaded bronzes from different vassal states; **c**, **d**: Comparison with binary bronzes from different vassal states

for the leaded bronzes are associated with the source of lead, therefore, this indicates possible lead circulation between the Baidian and Xincun areas and the above vassal states during this period.

If only binary bronzes (with < 2% Pb) are considered (Table S5), the lead isotope values of the bronzes are likely associated with copper. In Fig. 8c, d, areas A and C contain available lead isotope data of binary bronzes in Central China and Southern regions respectively, suggesting significant differences present in the sources of copper materials in the two regions [52, 62, 65, 68]. The Baidian slag data falls in area B, which contains lead isotope data of binary bronzes from both the Central China and Southern region. Area B is located between areas A and C, therefore, it could be resulted from mixing copper materials from areas A and C [69], or using copper ores available to the vassal states in Central China and Southern regions. The presence of area B reflects the circulation of copper materials between Jin, Qi, and Chu states, etc. (Fig. 8c, d). Although that only one Baidian slag data falling in area B is not sufficient to conclude that the bronze produced in Baidian were made using a mixture of copper materials from different sources, this hypothesis cannot be ruled out.

Lead and copper sources used in the Baidian and Xincun sites

The fifth to fourth centuries BCE were the prosperous stage of bronze production in the Jin state. Baidian was the representative of a large-scale bronze casting workshop during this period, and its material source is an important research issue. The material circulation between the Jin and other states helps us explore the sources of lead and copper materials at the Baidian and Xincun sites. Since Chu (located in middle and lower reaches of the Yangtze River) and Qi (in Jiaodong areas) had a vast territory during the Warring States period,

and previous studies have shown lead ore sources present within their borders [70, 71]. Thus, we carried out kernel density estimation analysis method to compare the lead isotope data of slags from the Baidian and Xincun sites and lead ores from the middle and lower reaches of the Yangtze River and Jiaodong areas. Additionally, lead isotope data of lead ores from the Xiaoqinling, Inner Mongolia and Yunnan-Sichuan regions adjacent to the Sanjin region were also included for the comparison (Fig. 9a–f). The lead isotope database of lead ores in mainland China collected by Hsu and Benjamin were cited here [72]. The lead isotope data of Jin leaded bronzes from different periods (Table S6) were also plotted in Fig. 9a-f to discuss the chronologic change in the use of the lead source by the Jin state [7, 52, 53, 73, 74].

As shown in Fig. 9, the lead isotope data of ores from the middle and lower reaches of the Yangtze River, and the Jiaodong region partially overlap with the data of the Baidian and Xincun slags. However, only the core density data center in the Xiaoqinling region showed the best

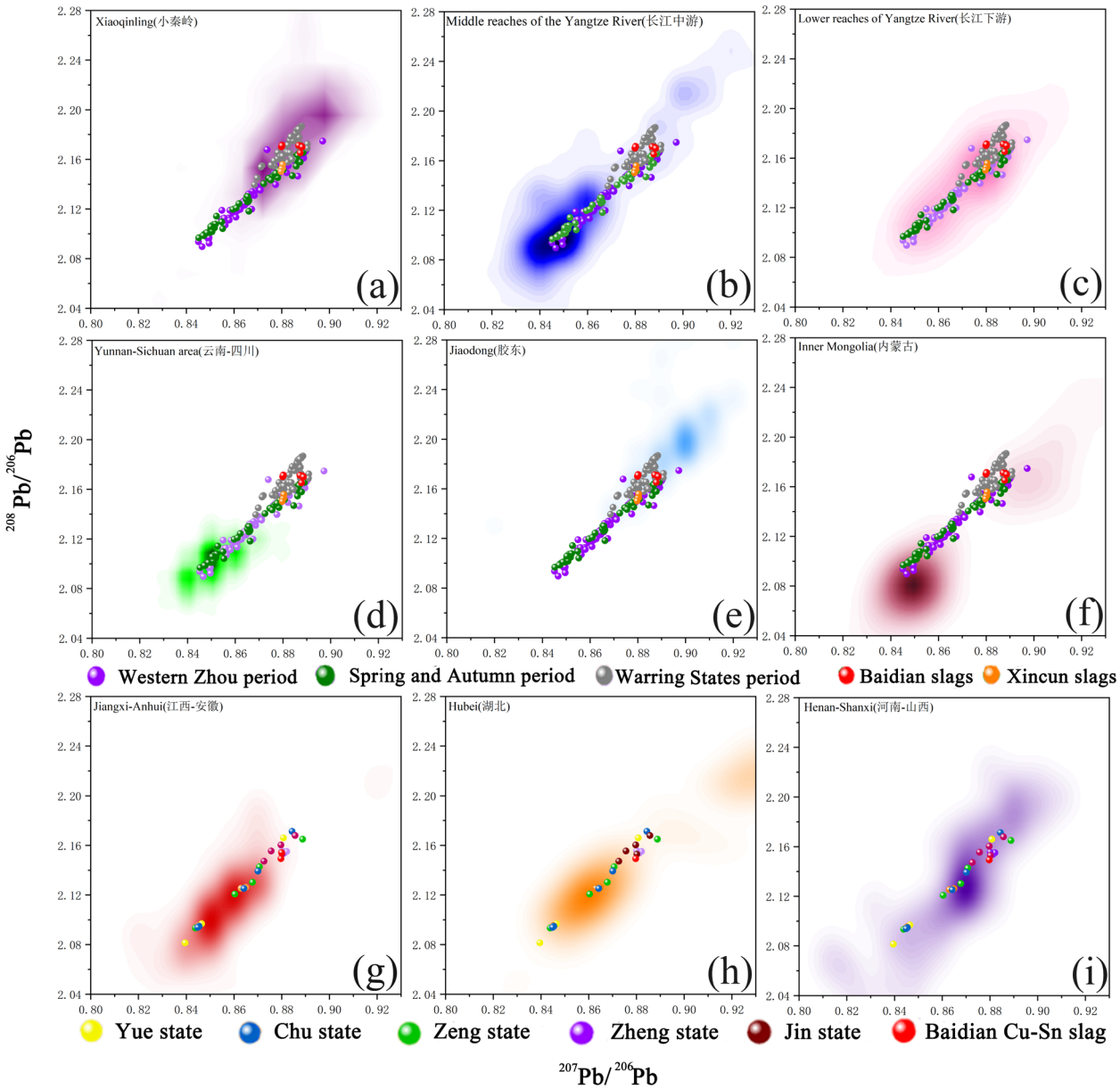

Fig. 9 Kernel density diagram comparing lead isotopes of Xincun and Baidian slags with lead, copper ores from various regions; **a**-**f**: Comparison of Cu-Sn–Pb slags with Jin bronzes from different periods (Table S6) and lead ores; **g**-**i**: Comparison of Baidian Cu-Sn slag with binary bronzes (Pb < 2%) from different vassal states (Table S5) and copper ores (modified from Yang et al., 2023)

match with the data of the slags (Figs. 9a), suggesting the lead material used at the Baidian and Xincun sites mainly came from the Xiaoqinling area. The Xiaoqinling area was a settlement of the Di during the Spring and Autumn period. The use of lead material in the Jin state may be related to the fact that after the Jin destroyed Di in the late Spring and Autumn period, the Xiaoqinling area was incorporated into the territory of Jin and local mines were developed [75].

In this study, slag BH20:044 from Baidian may provide information on the provenance of copper at the Baidian site. Chinese copper mines are mainly located in the Jiangxi-Anhui, Hubei, Henan-Shanxi, Yunnan, and Gansu region, copper mining and smelting sites during the Eastern Zhou era mainly have been discovered in the Jiangxi-Anhui, Hubei, and Henan-Shanxi regions [76]. Thus, the lead isotope data of copper ores in the above region were selected for comparison with the lead isotope data of slag BH20:044 and low-lead (< 2%) Jin bronzes [72] (Fig. 9g–i).

The data of slag BH20:044 and Jin bronze matches well with the copper ore data located in the Henan-Shanxi region (Fig. 9i), suggesting that the copper could have originated from the Henan-Shanxi region. A large number of ancient copper mining and metallurgical sites in the Henan-Shanxi region are mainly distributed in the Zhongtiaoshan area. As the closest copper source to Central China, the Zhongtiaoshan mining area is the most likely source of copper used at the Baidian [28]. However, the overlap of Jin binary bronze with marginal data from the Jiangxi-Anhui region and Hubei region makes it impossible to rule out these regions as potential copper sources (Fig. 9g, h). Since the mixing of raw copper from different sources during the smelting process also makes it difficult to determine the copper source [33], more copper isotope data and trace element data of copper slag samples are needed to further explore the copper materials source at the Baidian site in the early Warring States period.

Various factors influencing bronze production technology

The analysis results of the slags from the Baidian and Xincun sites reveal coexistence of various bronze production technologies at both the sites. The bronze production is not only constrained by technology but are also affected by resources, cost and production efficiency.

The use of metallic lead and copper for alloying is a common choice in the Baidian and Xincun sites, which may have resulted from the bronze production tradition in Central China. The main lead sources for Jin bronzes moved to the Xiaoqinling area from the middle and lower reaches of the Yangtze River during the Warring States period (Fig. 9a–c). The Xiaoqinling area is rich in lead resources and is located in the Jin, which has geographical advantages. It was easier for Jin to utilise local mineral resources, greatly reducing the cost of long-distance transportation of lead from the middle and lower reaches of the Yangtze River. At the same time, the Henan-Shanxi region was also able to provide adequate copper material for bronze production. Considering the established tradition of separate smelting and casting in Central China, copper and lead ingots have likely been produced at smelting sites and then transported to casting workshops [27, 28]. The discovery of lead ingots at the Baidian support the use of metallic lead for alloying [36]. In this paper, the copper ingots melting or refining occurred at both the sites were exemplified by slag BH2:07 and slag H91:4, respectively. Additionally, the remelt of waste bronze (e.g., slag BH2:09) also reduced metal losses and cut down the cost of bronze production.

The main difference between the Baidian and Xincun sites is reflected in the alloying techniques of tin materials. Baidian slag BH20:044 and BH20:045 showed melting copper with metallic tin, while Xincun slag H98:3 may indicate an alloying method by melting copper with tin ore. The emergence of the Bronze Age in Central China can be traced back to the Erlitou period, c. 1750–1520 BCE [77]. Most of slags of this time were melting slags, resulted from adding tin ore to metallic copper for bronze production [78–80]. The slags found during the Shang dynasty reflected a technological shift towards the use of tin ingots in bronze production, though no tin ingots have been discovered [27, 81]. The alloy technology became mature by the Zhou dynasty. Thus, the technical difference at both the sites may have caused by tin material availability and tin recovery. Tin-bearing minerals have been documented present in the Central China in pre-Qin inscriptions and ancient books [82–84], but no archaeological evidence have been found in Central China up to date. The acquisition of tin materials could have mostly relied on the southwest or southeast region of China by trade using lead materials [85, 86]. However, tin materials in the Jin state have probably decreased with the shift of copper and lead sources in the Jin state during the Warring States period. As a dependent state of the Jin, the circulation and distribution of tin materials in Wei has likely been more limited. As such, in order to reduce costs and improve production efficiency, Wei had chosen to add tin ore directly to alloying, ensuring a higher tin recovery by reducing the oxidative tin losses during smelting [87]. In contrast, metallic tin was still used in alloying in Jin for a better control of alloy compositions.

Conclusions

In this paper, slags and technical ceramics from the Baidian and Xincun foundry sites of different historical contexts were studied to explore the bronze production technologies and bronze material source at both the sites. A comparison of the differences and/or similarities in bronze production process between the two sites was made. The results show the following:

Slags from the Baidian and Xincun sites provide new information on the bronze production technology during the Eastern Zhou dynasty in the Sanjin area. This research shows distinctive bronze production techniques of the two foundries: in the Baidian site, bronzes were probably produced by co-melting of metallic copper and tin, as well as by remelting recycled bronzes. Although Wei state was politically attached to Jin, in the Xincun site, bronzes were probably made by co-melting of copper and tin ore.

The significantly different distribution in lead isotope ratios between the low-lead prills and high-lead prills revealed the provenance of copper and lead materials in the slag, respectively. The copper material used at the Baidian site may have come from Henan-Shanxi areas. The lead material used at the Baidian and Xincun sites may have come from the Xiaoqinling area.

The study demonstrates the importance of integrating resource networks and political contexts to interpret the bronze production technology among regions, so as to better understand the relationships between metal resources, metallurgical technology, and social dynamics. It is hoped that this research would promote archaeometallurgical study among other regions and be applied to other Bronze Age cultures in the world.

Supplementary Information

The online version contains supplementary material available at https://doi.org/10.1186/s40494-024-01449-1.

Additional file 1.

Acknowledgements
This research was supported by the National Natural Science Foundation of China (No. 52072220). The authors would like to thank Professor Rongyu Su of the Institute for the History of Natural Sciences, Chinese Academy of Sciences, for providing the samples for this study and his support of this project.

Author contributions
Quanyu Wang provided support and guidance for this study; Cong Wang performed all the experiments test, interpreted the data and wrote the manuscript; Quanyu Wang, Zhenlong Gao, Qingzhu Wang and Jun Gao revised this manuscript. All authors read and approved the final manuscript.

Funding
This study was supported by the National Natural Science Foundation of China (No. 52072220).

Availability of data and materials
No datasets were generated or analysed during the current study.

Declarations

Competing interests
The authors declare no competing interests.

Received: 6 May 2024 Accepted: 8 September 2024
Published online: 17 September 2024

References

1. Shanxi Provincial Institute of Archaeology. Art of the Houma foundry. New Jersey: Princeton university Press; 1996. p. 36.
2. Shanxi Provincial Institute of Archaeology. Houma baidian zhutong yizhi (Bronze foundry at Baidian, Houma). Beijing: Science Press; 2012. p. 284–8.
3. Chase WT, et al. Lead isotope ratios, in Eastern Zhou ritual bronzes from the Arthur M. Sackler collections, Jenny F., Published by the Arthur M. Sackler Foundation in association with the Arthur M. Sackler Gallery, Smithsonian Institution. 1995; 489–492.
4. Chase WT, Wang QY. Metallography and corrosion product studies on archaeological bronze fragments from the Qu Cun Site. MRS Online Proc Libr. 1996. https://doi.org/10.1557/PROC-462-73.
5. Chen KL, Mei JJ. Bronze vessels unearthed from Tomb A and B of Liulice, Huixian County scientific analysis research. Cult Rel Central China. 2011;06:99–105.
6. Han BH, Cui JF. A scientific analysis of the bronzes from the Fenshuiling Cemetery of the Eastern Zhou period in Changzhi. Shanxi Archaeology. 2009;07:80–8.
7. Nan PH. Research on bronzes technology of Jin kingdom in Spring and Autumn period. PhD Thesis, University of Science and Technology Beijing: Beijing.2017.
8. Nan PH, Wang XY, Qian W. Technical characteristics and related issues of bronze vessels unearthed from Wayaopo Cemetery M23 in Xi County, Shanxi province. Cult Rel Central China. 2019;01:114–9.
9. Wang QY. Metalworking technology and deterioration of Jin bronzes from the Tianma-Qucun site, Shanxi China. Mater Sci. 2002. https://doi.org/10.30861/9781841714042.
10. Zhang DY, Li YX, Guo YT. Preliminary scientific analysis of bronze artifacts unearthed from the Zhonghuo Cemetery, Dingxiang County of Shanxi province China. Sci Conser Archaeol. 2016;28(01):7–17.
11. Chen XS. An analysis of the antique patterns found at the Houma copper casting site in Shanxi. Cultural Relics. 2022;05:56–62.
12. Sun S, Qin Y, Zhang SY, et al. Surface treatment technique of pottery moulds in Houma site. Foundry. 2008;10:1037–40.
13. Tan DR. Research on the materials and processing techniques of Houma's pottery models from the Eastern Zhou dynasty. Archaeology. 1986;04:355–62.
14. Wang QY. Identification of surface coatings on ceramic bronze-casting moulds from the Houma foundry, Shanxi China. J Archaeol Sci Rep. 2023;48:1–12. https://doi.org/10.1016/j.jasrep.2023.103858.
15. Yang H. Study on the classification of pottery molds unearthed from the Houma copper casting site. Master Thesis. Shannxi normal university, Xian. 2015.
16. Chen K. The archaeological research on the Wei in the Western Zhou dynasty: Based on the sites and tombs of Wei region. PhD Thesis. Zhengzhou University: Zhengzhou. 2019.
17. Shanxi Provincial Institute of Archaeology. Bronze foundry sites at Houma. Beijing: Cultural Relics Press; 1993. p. 5.
18. Gao ZL. Xincun settlement Site, Hebi. Henan Popular Archaeol. 2019;06:16–7.
19. Gao ZL, Niu HB, Han CH. 2014 excavation of Western Zhou cemetery at Xidapo, Xincun site, Hebi. Henan pronvince Huaxia Archaeol. 2020;03:3–22.
20. Gao ZL, Tian SY, Niu HB. Excavation of Western Zhou Tombs at Xincun Site, Hebi, Henan province, in 2015. Huaxia Archaeol. 2022;05:37–48.
21. Martinon-Torres M, Rehren T. Technical ceramics. In: Roberts BW, Thornton CP, editors. Archaeometallurgy in Global Perspective. Springer: London; 2014. p. 107–31.

22. Lin J, Yang A, Lin R, et al. Review on *in situ* isotopic analysis by LA-MC-ICP-MS. J Earth sci. 2023;6:1663–91. https://doi.org/10.1007/s12583-023-2002-4.
23. Yu HX, Zhang YH, Liu XJ, et al. Improved *in situ* analysis of lead isotopes in low-Pb melt inclusions using laser ablation–multi-collector–inductively coupled plasma–mass spectrometry. Rapid Commun Mass Spectrom. 2022;22: e9383. https://doi.org/10.1002/rcm.9383.
24. Chen KY, Chao F, Yuan HL, et al. High-precision *in situ* analysis of the lead isotopic composition in copper using femtosecond laser ablation MC-ICP-MS and the application in ancient coins. Spectrosc Spect Anal. 2013;5:1342–9. https://doi.org/10.3964/i.issn.1000-0593(2013)05-1342-08.
25. Yuan HL, Chen KY, Bao ZA, et al. Determination of lead isotope compositions of geological samples using femtosecond laser ablation MC-ICPMS. Chin Sci Bull. 2013;32:3914–21.
26. Julia ML, Lgnacio MR, Pere CM, et al. Traditions and innovations: versatility of copper and tin bronze making recipes in Iron Age Emporion (L'Escala, Spain). Archaeol Anthropol Sci. 2020;12:124. https://doi.org/10.1007/s12520-020-01081-7.
27. Cui CP, Dai XM, Tian W. Copper smelting technology in the southern Jin region during the Xia and early Shang Dynasties: the example of the Xiwubi site in Jiangxian County. Shanxi Archaeol. 2022;07:98–108.
28. Li YX. Preliminary investigation and research on ancient copper mining and metallurgy sites in Zhongtiao Mountain. J Chinese Antiquity. 1993;2:64–7.
29. Mao O, Dahn JR. Mechanically alloyed Sn–Fe(-C) powders as anode materials for Li-ion batteries. II. The Sn–Fe system. J Electrochem Soc. 1999;146(2):414–22.
30. Farci C, Martinón-Torres M, González-Álvarez D. Bronze production in the Iron Age of the e Iberian Peninsula: The case of *El Castru*, Vigaña (Asturias, NW Spain). J Archaeol Sci Rep. 2017;11:338–51. https://doi.org/10.1016/j.jasrep.2016.12.009.
31. Su ZJ. Research on the behaviour of tin removal from tin-bearing iron ores by reduction roasting. MA Thesis, Central South University, Changsha. 2014.
32. Rademakers FW, Rehren T. Seeing the forest for the trees: assessing technological variability in ancient metallurgical crucible assemblages. J Archaeol Sci. 2016;07:588–96. https://doi.org/10.1016/j.jasrep.2015.08.013.
33. Liu S, He XL, Chen JL, et al. Micro-slag and "invisible" copper processing activities at a Middle-Shang period (14th-13th century BC) bronze casting workshop. J Archaeol Sci. 2020;122:105–222. https://doi.org/10.1016/j.jas.2020.105222.
34. Elin F, Rui JCS, João CSM, et al. Smelting and recycling evidences from the Late Bronze Age habitat site of Baiões (Viseu, Portugal). J Archaeol Sci. 2010;37:1623–34. https://doi.org/10.1016/j.jas.2010.01.023.
35. Rademakers FW, Farci C. Reconstructing bronze production technology from ancient crucible slag: experimental perspectives on tin oxide identification. J Archaeol Sci Rep. 2018;18:343–55. https://doi.org/10.1016/j.jasrep.2018.01.020.
36. Shanxi Provincial Institute of Archaeology. Houma zhutong yizhi (Bronze foundry sites at Houma). Beijing: Cultural Relics Publishing House; 1993. p. 413.
37. Li HC, Cui JF, Zhou ZQ, et al. The production of the bronze weapons unearthed from the eastern Zhou burials at the Xinghe road locality of Jinsha site in Chengdu. Archaeology. 2018;07:87–95.
38. Pollard AM, Bray PJ. A new method for combing lead isotope and lead abundance data to characterize archaeological copper alloys. Archaeometry. 2015;57(6):996–1008. https://doi.org/10.1111/arcm.12145.
39. Craddock PT. Early Metal Mining and Production. Edinburgh University Press: Edinbergh.
40. Bachmann HG. The identification of slags from archaeological sites. London: Institute of archaeology; 1995.
41. Bourgarit D, Mille B. Were the first metallic objects produced by metallurgists. L'Actualité chimique, 2007; 54–60.
42. Liu S, Rehren T, Pernicka E, et al. Copper processing in the oases of northwest Arabia: technology, alloys and provenance. J Archaeol Sci. 2015;53:492–503. https://doi.org/10.1016/j.jas.2014.10.030.
43. Rovira S. 2007 La producción de bronces en la Prehistoria. In: Molerai Marimon J, Farjasi Silva J, Rourai Grabulosa P, Pradelli Cara T (eds). Avances en Arqueometría 2005. Actas Congreso Ibérico de Arqueometría. Universitat de Girona: Girona. 21–35.
44. Renzi M. La Fonteta (Guardamar del Segura, Alicante) y la metalurgia fenicia de época arcaica en la Península Ibérica. PhD Thesis, Universidad Complutense de Madrid. 2013.
45. Mao JW, Ouyang HG, Song SW, et al. Geology and metallogeny of tungsten and tin deposits in China. Soc Econ Geol. 2019;22:411–82.
46. Zhang JB, Ding JH, Nan GL. The characteristics and potential of tin resources in China. Geol China. 2015;42(04):839–52.
47. Zhang ZB, Sun LQ. Geological characteristics and ore controlling factors of tin deposits. Mineral resources. 2021; 105–106.
48. Zhao YM, Feng CY, Li DX. New progress in prospecting for skarn deposits and spatial-teporal distribution of skarn deposits in China. Mineral Deposits. 2017;36(03):519–43.
49. Chen SC, Yu JJ, Bi MF, et al. Tin-bearing minerals at the Furong tin deposit, South China: Implications for tin mineralization. Geochemistry. 2021;82(01): 125856. https://doi.org/10.1016/j.chemer.2021.125856.
50. Li CY, Li YX, Wang LX, et al. Archaeometallurgy Study on the Relics Excavated from the Habaqila Site in Keshiketeng Banner. Inner Mongolia Jianghan Archaeol. 2023;4:122–30.
51. Tao ZG. Tomb of Zhao Qing of Jin State in Taiyuan. Beijing: Cultural Relics Press; 1996. p. 253–69.
52. Tan JZ, Wu XT, Fan WQ, et al. A study on the metal ore source of the early warring states bronzes unearthed from tomb M5001 at Qiujiazhuang cemetery of Wenxi county. J Nat Museum China. 2023;04:88–98.
53. Yang YL. Study on the alloy composition, microstructure and lead isotope ratio of bronzes from the Jin Marquis Cemetery in Northern Zhao. Master Thesis. Peking University, Beijing. 2005.
54. Zhang XT. Study on the technological characteristics and mineral source of bronzes unearthed in Wenxi, Shanxi. Master Thesis. Shandong University: Qingdao. 2024.
55. Wen RJ. Artificers´ records (Kaogongji). Shanghai: Shanghai Classics Publishing House; 2021. p. 43–5.
56. Gale ZS, Gale NH. Lead isotope analyses applied to provenance studies, in modern analytical methods in art and archaeology: chemical studies series. New York: John Wiley&Sons Inc; 2000. p. 503–84.
57. Yu YB, Chen JL, Mei JJ. Several issues regarding the study of lead isotope ratios in Yejiashan bronzes. Cult Rel Southern China. 2016;01:94–102.
58. Jin ZY. Lead isotope archaeology in China. Beijing: University of Science and Technology of China Press; 2008. p. 185.
59. Rademakers FW, Verly G, Somaglino C, et al. Geochemical changes during Egyptian copper smelting? an experimental approach to the Ayn Soukhna process and broader implications for archaeometallurgy. J Archaeol Sci Rep. 2020;122:105–223. https://doi.org/10.1016/j.jas.2020.105223.
60. Hao DH, Zhang J, Du XJ, et al. Analysis of Eastern Zhou Bronzes Unearthed at Dubei Cemetery. J Nat Museum China. 2021;06:111–21.
61. Zhang J, Sun B, Hao DH, et al. Chronological research and scientific analysis on bronzes unearthed from ancient City Site of the Xue state in Tengzhou, Shandong. J Nat Museum China. 2020;10:98–114.
62. Wang YC, Zhang J, Lei S, et al. Preliminary scientific analysis on the Bronze Wares Unearthed from the Yushan Site in Zhenhai District, Ningbo City. Cult Rel Southern China. 2019;03:114–21.
63. Zhang J. A Study of the Resources and Technology of Eastern Zhou Bronzes - Focusing on the Hanhuai Region. PhD Thesis. Peking University: Beijing. 2020.
64. Li HC, Cui JF. Circulation of Copper between the Jin and Chu states: a synthetical analysis of technologies bronze inscriptions, and archaeological remains. Archaeol Cult Rel. 2018;02:96–101.
65. Li HC, Zuo ZQ, Cui JF, et al. Copper alloy production in the Warring States period (475–221 BCE) of the Shu state: a metallurgical study on copper alloy objects of the Baishoulu cemetery in Chengdu China. Herit Sci. 2020;67(8):1–16. https://doi.org/10.1186/s40494-020-00412-0.
66. Luo Z, Jin ZY, Hu GH, et al. Lead isotopes of Eastern Zhou bronzes unearthed from Shaoyang of Hunan. Jianghan Archaeol. 2023;03:125–33.
67. Jia LJ, Yao Y, Zhao CC, et al. Mineral sources of lead aggregate about early Qin bronze wares. Stud Hist Nat Sci. 2015;34(01):97–104.
68. Li Q, Huang HY, Li LX, et al. Lead isotope ratio analysis of several Zhou dynasty bronzes unearthed in Northern Anhui province. Rock Mineral Anal. 2022;41(01):14–21.
69. Cui CP, Tang YY, Tian W, et al. A study on copper slag unearthed from Eastern Zhou Dynasty remains at the Xiwubi site in Jiangxian County, Shanxi Province. J Nat Museum of China. 2021;08:79–87.

70. Cui CP, Li YX, Dai QL. Analysis on the resource provenance for mineral materials of bronzes and the slags in Shandong Peninsula. Cult Rel Southern China. 2021;03:184–90.
71. Liu ZF, Ma JC, Wang CM, et al. A lead isotope study of the fourth century B.C. bronze artifacts excavated from Guozhuang Chu graveyard in Shangcai County, Henan Province Central China. Archaeol Anthropol Sci. 2019;11:759–2769. https://doi.org/10.1007/s12520-018-0699-2.
72. Hsu YK, Benjamin JS. A geochemical characterization of lead ores in China: an isotope database for provenance archaeological material. PLoS ONE. 2019;14(4): e0215973. https://doi.org/10.1371/journal.pone.0215973.
73. Group of Shang and Zhou dynasties. Archaeology department, Peking University and Shanxi Provincial Institute of Archaeology. Beijing: Tianma-Qucun Science Press; 2020.
74. Nan PH, Gao ZH, et al. Reconsideration on the material, technology and mineral characteristics of the bronze wares in the Eastern Zhou period cemetery of Fenshuiling. Cult Rel Southern China. 2021;3:191–9.
75. Li MC, Li SS. History of Jin, Sanjin Publishing House 2015; 493-495
76. Liu L, Chen X. City: the issue of control over natural resources in the Xia and Shang Dynasties. Southeast Culture. 2000;3:45–60.
77. Su RY, Hua JM, Li KM, et al. The metal technology of early ancient China. Jinan: Shandong Science and Technology Press; 1995. p. 38.
78. Li YX, Xu H. Preliminary study of the smelting and casting relics excavated from the Erlitou site. Beijing: Science Press; 2007. p. 59–82.
79. Liang HG, Li YX, Sun SY, et al. Study of the arsenic-bearing slag excavated from the Yuanqu City site. Nonferrous Metals. 2005;04:127–30.
80. Liang HG. Reflections on some special phenomena in the metallurgical relics excavated from the Erlitou site. Cult Rel Southern China. 2019;05:60–7.
81. Liang HG, Li YX, Sun SY, et al. Preliminary study of the metal particles and mineral composition within the furnace wall and slag excavated from the Yuanqu City site. Sci Conser Archaeol. 2009;21(04):18–30.
82. Shi ZR. Bronze casting technology in the Yin dynasty. Acad Sinica Hist Lang Res Inst J. 1955;26:95–129.
83. Wen G. Ancient bronze and tin mines in the Central China. Geol Rev. 1980;04:331–40.
84. Li YX. "Records of local products of china post" records Shanxi's tin production and its significance collection of essays on the history of Chinese metallurgy. Beijing: Science Press; 2006. p. 359–66.
85. Jin ZY. On the highly radiogenic lead in bronzes of the shang dynasty archaeology academic journal. Beijing: Relics Press; 2004. p. 269–78.
86. Yi DS. The source of tin and the "Copper-tin Road" of the Shang dynasty in the perspective of archaeometry. Soc Sci China. 2003;5:162–84.
87. Charles JA. The development of the usage of tin and tin-bronze: some problems. In: Olin JS, Wertime TA (eds) Franklin AD. The search for ancient tin, Washington. 1978; 25–32

Publisher's Note